PHYSICAL REVIEW B VOLUME 12, NUMBER 4 15 AUGUST 1975

Current transport in relaxation-case GaAs

M. Ilegems and H. J. Queisser*
Bell Laboratories, Murray Hill, New Jersey 07974

(Received 22 July 1974)

Current-voltage characteristics of p-ν-n structures, where the ν region is oxygen-doped relaxation-case GaAs, have been redetermined with particular attention given to the characterization of the contacts to the high-resistivity ν layer. The forward characteristics exhibit near-Ohmic behavior up to applied voltages that are considerably larger than the built-in potential, which is then followed by a range of sublinear increase of current with voltage. These results are consistent with earlier observations and provide evidence that the characteristics are determined by a space-charge region of increased resistance adjoining the injecting p contact. The results are discussed in relation to the relaxation-case theory which ascribes the sublinear current increase to the growth of this space-charge region by recombinative injection, i.e., depletion of the majority carriers through recombination with the injected minority carriers before dielectric relaxation can occur. Questions regarding this interpretation and its implications regarding relaxation-case recombination and trapping are discussed.

I. INTRODUCTION

The electronic properties of amorphous materials[1,2] have recently been analyzed[3] on the basis of the theoretical approach based on the unifying concept of the relaxation semiconductor.[4–7] High-resistivity crystalline semiconductors constitute a class of relaxation-case materials whose electrical properties are generally better defined than those of the amorphous films. Their study therefore provides an important means for detailed analysis of some of the novel concepts of relaxation-case behavior.

The relaxation case obtains when the dielectric relaxation time $\tau_D = \rho\epsilon$, where ρ is the resistivity and ϵ the dielectric constant of the material, exceeds the carrier diffusion-length lifetime τ_0. The opposite inequality holds for the conventional or lifetime-case semiconductor. In the relaxation case the usual condition of local electrical neutrality is no longer obeyed and replaced by the condition of near-zero net local recombination in space-charge regions whose decay depends on dielectric relaxation.

A principal result of the analysis by van Roosbroeck[5] of carrier transport in relaxation-case semiconductors is the prediction of recombinative injection. This effect is manifested by reduction of the density of majority carriers through injection of minority carriers. In an extrinsic semiconductor increase of resistance can result, which is quite contrary to the decrease in resistance always observed in the lifetime case. Recombinative injection is predicted as a direct consequence of the characteristic relaxation-case approximation for an injected region, namely, that the excess of the local recombination rate over the thermal-equilibrium generation rate is relatively small so that the concentration product np retains its thermal equilibrium value n_i^2.

Diodes consisting of oxygen-doped semi-insulating GaAs with a diffused Zn-doped p contact were used in the initial relaxation-case transport experiments.[5] These experiments showed a sublinear current-voltage characteristic for a forward-biased p-n junction, which was cited as evidence for recombinative injection. Potential-probing experiments[6] did indeed later confirm that most of the voltage drop and resistance are across a space-charge layer which adjoins the p contact and widens with increasing bias. As originally proposed,[5] such sublinear dependence may be expected to result from the widening of this layer through progressive removal of majority electrons from the bulk in accord with the characteristic approximation $np = n_i^2$.

Considerable controversy[8–10] arose later concerning various aspects of the theory. Additional experiments therefore seemed necessary, and form the subject of the present paper. We treat first the problems of characterizing the electrical behavior of high-resistivity materials and examine the effects of contact-related space-charge layers on the over-all transport properties. Then, well-defined GaAs samples are used to further investigate the sublinear forward characteristic in its relation to the proposed recombinative injection. Finally, the interpretation of the data is discussed.

II. EXPERIMENTAL

Three types of high-resistivity GaAs were used: (a) oxygen-doped GaAs, grown at Bell Laboratories by the floating-zone (fz) technique in an oxygen-containing atmosphere, the same material used in the previous experiments by van Roosbroeck and Casey[5] as well as by Queisser *et al.*[6]; (b) oxygen-doped boat-grown (bg) GaAs obtained from Monsanto Co.; and (c) chromium-doped boat-grown crystals obtained from Laser Diode Laboratories. These crystals are usually weakly *n*-type with $\rho \approx 10^8$ Ω cm at 300 K; we describe this conductivity as *ν* type.

Hall measurements were made by standard dc techniques on disc-shaped samples using the Van der Pauw[11] configuration. The temperature range was from 40 to 200 °C. Voltages were read using a Keithley 602 electrometer with 10^{16}-Ω input impedance. The contacts were made by capacitor discharge bonding of 95%-Au–5%-Sn wires to the crystals. Over the temperature range of the measurements these contacts appeared Ohmic as determined from the symmetry of the Hall voltages upon reversal of current or field, or from the curve tracer display of their current-voltage characteristics. It was also verified that the Hall results were not influenced by surface conduction by repeating some measurements after the samples had been thinned down from 400 to 100 μm and reetched.

Current-voltage characteristics were measured on symmetrical *n-ν-n* structures and on *p-ν-n* diodes. Three types of *n-ν-n* structures were prepared: (i) by successive evaporation of Sn (≈ 5000 Å layer), Pt (≈ 2500 Å), and Sn (≈ 5000 Å) onto a freshly etched substrate at 150 °C in vacuum, followed by alloying *in situ* at 525 °C for 20 sec; (ii) by growth of a Sn-doped ($n \approx 5 \times 10^{18}$ cm^{-3}); or (iii) of a Te-doped ($n \approx 5 \times 10^{18}$ cm^{-3}) GaAs layer by liquid-phase epitaxy (LPE) between 800 and 780 °C, after which final contacts were made by Sn-Pt-Sn evaporation as per (i) above. For the *p-ν-n* structures the *p* injector contact was formed by closed-ampoule Zn diffusion from a ternary 5-, 50-, and 45-at.% Ga, As, and Zn diffusion source[12] at 650 °C for 8 h. By cleaving and etching the diffusion depth was measured to be 3 ± 1 μm; surface concentration is expected to be $p \approx 10^{20}$ cm^{-3}. For these samples the back contact was grown first by LPE using Sn as the dopant. After Zn diffusion, the back contact was then etched to remove the Zn-diffused surface layer prior to performing the final Sn-Pt-Sn evaporation and alloying.

Samples were in the form of square slabs of 0.75-mm side as obtained either directly by cleaving or else by sawing followed by etching with bromine-methanol to remove surface damage. The characteristics were measured with the samples in a shielded dark enclosure, using Keithley 602 and 616 electrometers. The leakage resistance of the apparatus with samples removed was greater than 5×10^{12} Ω, more than two orders of magnitude in excess of any measured sample impedance.

III. ELECTRICAL CHARACTERIZATION

A. Conductance data

A series of *n-ν-n* structures was evaluated to verify the linearity of the contacts and to obtain the resistivity of the material in addition to that derived from Hall effect data. Current-density (*J*)–voltage (*V*) characteristics varied considerably with contacting procedures. Structures with Sn-doped epitaxial or evaporated contacts consistently showed Ohmic behavior at low fields followed by a superlinear *J*-*V* dependence. Figure 1 shows typical room-temperature measurements. The examples chosen are for evaporated contacts; similar results were found for epitaxial-layer contacts. We regard the absence of sublinearity in the *J*-*V* curves as evidence for absence of space-charge layers near the contacts which under reverse bias would yield a noticeable sublinear behavior. For all oxygen-doped crystals with Te-doped contacts [method (iii)] however, the *J*-*V* characteristic often showed extended sublinear regions where *J* was proportional to $V^{1/2}$. This contacting method was therefore rejected. The reason for the difference in behavior between group-IV and group-VI donors is presently not understood.

The temperature dependence of the resistivities, determined in the Ohmic region of the characteristics, is displayed in Fig. 2. Also included in

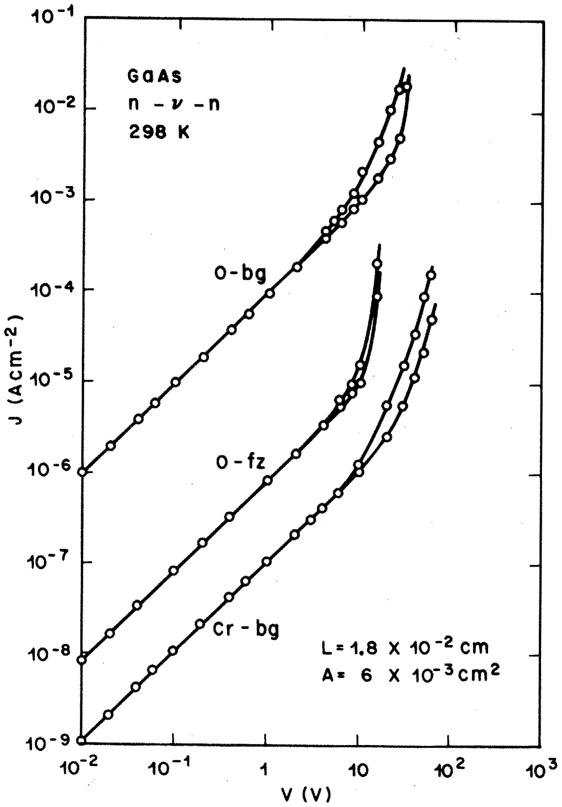

FIG. 1. Current-density–voltage characteristics: *n-ν-n* structures with Sn-Pt-Sn alloyed *n* contacts. The characteristics are linear and symmetric with respect to voltage polarity in the low-field region before the onset of superlinearity.

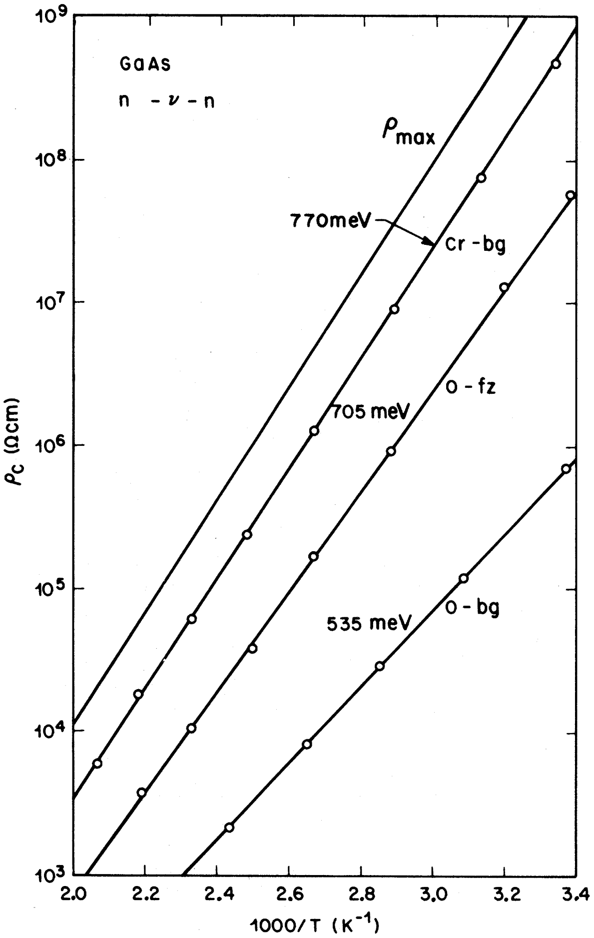

FIG. 2. Resistivity ρ_c vs inverse temperature from conductance data on n-ν-n structures with Sn-Pt-Sn-alloyed n contacts. Same samples as in Fig. 1.

TABLE II. 298-K resistivities and activation energies from conductance measurements.

Crystal	O−bg	O−fz	Cr−bg
ρ_c (Ω cm)	6×10^5	5×10^7	6×10^8
E_ρ (meV)	535 ± 10	705 ± 10	770 ± 10

this figure is the temperature variation of the maximum resistivity[5]

$$\rho_{\max}=[2en_i(\mu_n\mu_p)^{1/2}]^{-1}, \qquad (1)$$

where the intrinsic carrier concentration n_i is given by

$$n_i=(N_cN_v)^{1/2}\,e^{-E_g/2kT}. \qquad (2)$$

The parameters used for this calculation are listed in Table I.

TABLE I. Selected constants[a] for GaAs.

$E_g(\mathrm{eV})=1.424$	(298 K)
$E_g(T)(\mathrm{eV})=1.519-5.4\times10^{-4}T^2/(204+T)$	
$m_e=0.0665\ m_0$	
$m_h=0.5\ m_0$	
$N_c\ (\mathrm{cm^{-3}})=2\ (2\pi m_e kT/h^2)^{3/2}=8.3\times10^{13}\ T^{3/2}$	
$N_v\ (\mathrm{cm^{-3}})=2\ (2\pi m_h kT/h^2)^{3/2}=1.7\times10^{15}\ T^{3/2}$	
$n_i\ (\mathrm{cm^{-3}})=(N_cN_v)^{1/2}e^{-E_g/2kT}=1.8\times10^6$	(298 K)
$\rho_{\max}{}^{b}(\Omega\ \mathrm{cm})=[2en_i\ (\mu_n\mu_p)^{1/2}]^{-1}=2.9\times10^9$	(298 K)

[a] After Refs. 13 and 14.

[b] Assuming $\mu_n=3000\ \mathrm{cm^2/V\ sec}$, $\mu_n/\mu_p=20$.

The 298-K resistivities, ρ_c, determined from conductance data and their corresponding thermal-activation energies, are summarized in Table II. Good agreement was obtained between the resistivity values determined on several samples of the same material whose length and cross sections varied by up to a factor of 5. The values of Table II are therefore representative of the bulk properties of the crystal.

B. Hall-effect data

Results of Hall measurements on the three types of samples investigated are summarized in Table III. The electron concentration n and mobility μ_n were evaluated using the simplified expressions

$$n=(-eR_H)^{-1} \qquad (3)$$

and

$$\mu_n=-R_H/\rho_H, \qquad (4)$$

where e is the electronic charge, R_H the Hall coefficient, and ρ_H the Van der Pauw resistivity. It can be verified that Eqs. (3) and (4) constitute a valid approximation to the present results by inserting the values of R_H and ρ_H into the two-carrier expressions[15] for Hall coefficient and resistivity and solving for n and μ_n, assuming a reasonable value for the mobility ratio μ_n/μ_p. Such calculations show that even for the Cr-doped samples the electron concentration exceeds n_i by at least a factor of 2 throughout the temperature range. Predominant electron conduction is also indicated by the relatively large mobilities measured both in

TABLE III. Hall-measurements results.

Crystal	O−bg	O−fz	Cr−bg	
ρ (Ω cm)	4×10^6	1.5×10^8	5×10^8	(298 K)
E_ρ (meV)	700 ± 10	755 ± 10	765 ± 10	
n (cm^{-3})	7×10^8	1.4×10^7	4×10^6	(298 K)
E_d (meV)	610 ± 10	690 ± 10	···	(298 K)
E_a (meV)	···	···	745 ± 10	(298 K)
μ (cm^2/V sec)	2880–2640	3300–2500	2300–2080	(340–500 K)

O- and Cr-doped crystals.(Table III).

Oxygen forms a deep donor level in GaAs.[16] When the conductivity is controlled by a single deep donor level whose concentration N_d is much larger than the net contribution N_S due to shallower acceptor (N_A) and donor (N_D) levels ($N_S = N_A - N_D > 0$) the depth of the donor level below the conduction band can be obtained from the expression

$$\frac{d\ln(nT^{-3/2})}{d(1/T)} = -\left(E_d - \frac{TdE_d}{dT}\right)\bigg/k \qquad (5)$$

valid when $n \ll N_S \ll N_D$. Using the data of Table I and assuming that the *relative* position of the impurity level within the gap remains constant with temperature, we obtain $E_d(\text{O}) = (690 \pm 10)$ meV at 298 K, in approximate agreement with earlier determinations.[17,18] In cases of close compensation ($N_d \approx N_S$), the true ionization energy will be larger[19] than that obtained by the method outlined above. Such situation probably applies to the bg O-doped material; in this case, close compensation is also suggested by the fact that the mobilities of the bg crystals are lower than those of the fz crystals.

The characteristics of the O-doped fz crystals as determined by Hall measurements remained stable upon annealing of the crystals in a flow of H_2 at 800 °C for 4 h. The behavior of the O-doped bg crystals under various heat treatments, however, appeared somewhat erratic, again probably as a result of a higher degree of compensation or a lower O content in these crystals. For this reason, the discussion of diode characteristics in O-doped material is limited to fz crystals.

Chromium is generally assumed to be a deep acceptor in GaAs with an energy level very close to the intrinsic level. The crystals measured were n-type with the Fermi level lying slightly above the intrinsic level. In that case the acceptor ionization energy E_a is obtained from the temperature dependence of the carrier concentration by the equation

$$\frac{d\ln(nT^{-3/2})}{d(1/T)} = -\left(E_g - E_a - \frac{Td(E_g - E_a)}{dT}\right)\bigg/k \quad , \qquad (6)$$

valid when $N_a \gg N_S = N_D - N_A \gg n$, where N_a represents the deep acceptor concentration. Assuming again that the impurity level maintains a constant relative position within the gap, the result E_a (chromium) = 745 ± 10 meV (298 K) is obtained. This value is somewhat lower than a previous determination[20] in which the terms involving the band gap E_g and the temperature dependences of E_g and E_a were neglected.

C. Discussion of the electrical data

A significant result is the apparent discrepancy between Hall-effect measurements and conductance measurements on n-ν-n structures as shown by the distinctly different values of resistivity and activation energy displayed in Tables II and III. In the case of the O-doped crystals, the room-temperature resistivities determined from conductance measurements on n-ν-n structures are a factor of 3–6 lower than those derived from Hall data. More importantly, the resistivity activation energies from conductance data are substantially lower than those derived from the Hall measurements. No such discrepancy exists in the case of the Cr-doped crystals where both resistivities and activation energies from Hall data and conductance measurements are in quite close agreement.

The Hall data appeared entirely well behaved over the current and temperature ranges of our measurements. However, this apparently Ohmic behavior of the contacts does not exclude the existence of a depletion layer between the contact and the bulk, as evidenced for example by the extended linear regions found in the J-V characteristics of some of the p-ν-n diode structures discussed in Sec. IV. We conclude therefore, that the conductance measurements give us the correct bulk-resistivity values, while the Hall data may be obscured by space charge layers near the contacts. This conclusion demonstrates that all electrical data involving high-resistivity materials must generally be analyzed with caution in order to arrive at values which are truly representative of the material and are not influenced by contact conditions, even when seemingly linear J-V characteristics are observed.

The Cr-doped samples display very close agreement between the results of conductivity and Hall measurements. This suggests that any systematic experimental error in either set of measurements, such as could be caused, for example, by surface leakage across the n-ν-n structures, is not a major concern. In addition, this agreement shows that there is no evidence to suspect the presence of depletion layers adjacent to the contacts for the Hall samples in this case.

The energies listed in Table II are consistent with the value $E_d(\text{O}) = 790$ meV obtained from the spectral dependence of the photoionization cross section,[21] as well as with the values $E_d(\text{O}) = 750$ meV and $E_a(\text{Cr}) = 780$ meV obtained from transient capacitance measurements.[22] Appreciably smaller values for the Cr-acceptor binding energy have been deduced from photoconductivity data.[23,24]

IV. DIODE CHARACTERISTICS

A. Conditions for sublinear forward current

The material and diode configuration were chosen so as to satisfy a number of conditions for the observation of a sublinear forward characteristic caused by recombinative injection. First, the material must be extrinsic and its net doping level should be sufficiently low so that the condition $\tau_D \gg \tau_0$ will apply and that the injection level will not have to be too large. Second, the resistivity should be sufficiently less than $\rho_{\max}$, since otherwise a resistance increase becomes unobservable. This condition implies that O-doped GaAs with bulk resistivity about two orders of magnitude lower than $\rho_{\max}$ appears more likely to display any current sublinearity than the near-$\rho_{\max}$ Cr-doped material. Third, $\rho_{\max}$ itself should not be so large such that the depletion effect becomes completely masked by surface leakage.

Finally, the diodes should be of sufficient length such that the depletion region adjoining the injector contact does not already extend up to the opposite contact at zero bias. We note also that the less-mobile holes should preferably be injected into *n*-type material. When the mobility ratio is fairly large this choice[25] leads to a more drastic effect which should be easier to observe, since the more mobile carriers are removed. This last requirement suggests the use of *p*-*ν* structures rather than the complementary.

B. Back contacts

In view of the controversies following the previous experiments,[5,6] considerable effort was made to ensure that the diode characteristics measured were determined uniquely by the properties of the *p*-*ν* junction rather than by those of the back contact. This is especially important since a sublinear forward characteristic could result[8–10] simply from the presence of a reverse-biased rectifying back contact. This possibility can now be discounted. First, sublinear forward characteristics were observed, as will be discussed in Sec. IV C, with well-proven linear nonblocking contacts. Second, the effect was observed with mesa structures, where the *p* side was etched to yield mesas with orders-of-magnitude smaller areas, thus much larger current densities, near the junction than at the *n*-side back contact. This experiment verifies that the main resistance and most of the voltage drop occur near the injector contact. Further evidence that the device resistance is determined mostly by the junction region and that surface conduction is unimportant was obtained by varying the diode lengths and cross-sectional areas. The results indicate that length variations do not cause proportional variations in diode resistance, while the resistance scales inversely with area.

C. Diode characteristics–O-doped substrates

Characteristics were measured for samples of 400-, 800-, and 1600-μm total length having Zn-diffused *p* contacts and Sn-doped epitaxial back contacts. Results for these three series of samples were very similar. Measured characteristics for the $L = 400$ μm and $L = 1600$ μm samples are shown in Figs. 3 and 4, the data being representative of the results obtained on several diodes obtained from each substrate.

Some specific features of these results are discussed below:

(a) The forward characteristics of the diodes exhibit an extended linear region at low fields which is followed by a slightly superlinear region and then becomes markedly sublinear. In these Zn-diffused junctions sublinearity sets in at voltages from 40 V (short diodes) to 70 V (long diodes).

(b) The device resistance in the Ohmic low-field region is larger than that predicted on the basis of the bulk-resistivity value ρ_c (Table II) assuming uniform resistivity throughout the length of the sample. The difference in value is between a factor of 4–10, depending on sample length. This increased resistance indicates the presence of a high-resistivity layer near the junction which is even maintained under large forward bias. The width of this layer at zero or low bias can be es-

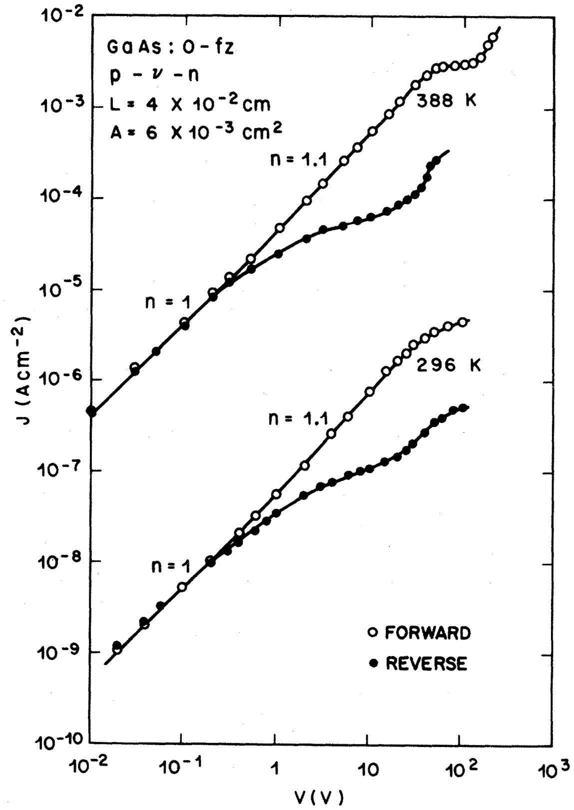

FIG. 3. Current-density–voltage characteristics: *p*-*ν*-*n* diode, Zn-diffused *p* contact, Sn-doped LPE *n* contact. Slopes in linear regions are designed by *n*.

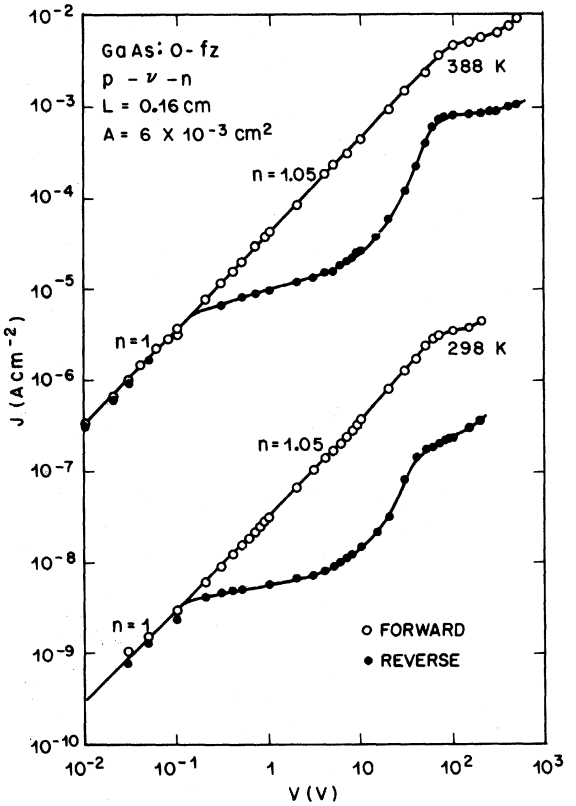

FIG. 4. Current-density–voltage characteristics: p-ν-n diode, Zn-diffused p contact, Sn-doped LPE n contact.

timated from the measured sample resistance assuming that the layer is depleted to resistivity $\rho_{\max}$. This estimate gives a minimum width w_m which ranges between 50 and 100 μm.

(c) The voltages at the onset of sublinearity increase with increasing space-charge layer width from 40 to 70 V.

(d) Over the temperature span of the measurements (~25 to ~120 °C) the shape of the characteristics remains largely unchanged. At constant applied voltage the forward currents scale with temperature according to thermal-activation energies from 720 to 780 meV.

(e) The sublinearity in the reverse characteristic starting at around 1 V is indicative of the usual depletion layer widening under reverse bias.[6] With increasing voltage the depletion layer widens until the resistivity of the entire crystal equals or becomes slightly larger than $\rho_{\max}$. At this point the characteristic continues with generally larger than unity slope to revert again to sublinear at high fields.

D. Transient response

In the sublinear forward and reverse regions the initial value of the current following the application of a voltage step corresponded closely to that expected[7] from a linear extrapolation along the Ohmic portion of the J-V characteristic. After this initial overshoot the current decayed approximately exponentially to its steady-state value. Time constants for this current decay, measured by recording the analog output of the current electrometer, were in the range from ~4 to ~15 sec in the sublinear reverse region. Time constants of the same order were observed along the sublinear forward branch. Decay time constants were largely independent of the amplitudes of the voltage steps except near the ends of the sublinear regions where the current decay becomes more rapid. For voltage increments within the Ohmic ranges of the characteristics the current response was rapid and without pronounced overshoot, showing thereby that the slow current decay is determined by sample response rather than circuit effects.

The time dependence of the current decay is determined[26,27] by the emission and capture rates of the impurity levels in the space-charge layers as well as by the resulting rate of widening of these layers. The time constants decreased with increasing temperature according to activation energies from 700 to 800 meV. Because of the limited temperature interval of our measurements (296–318 K) these energies are rather imprecise. However, they are suggestive of capture and emission by traps near the middle of the gap.

E. Diodes with Cr-doped ν-layer

p-ν-n structures with Sn-doped LPE n back contacts and Zn-diffused p contacts showed a behavior quite distinct from that observed in the O-doped crystals. Their J-V characteristics are displayed in Fig. 5. Forward and reverse characteristics are identical up to voltages of 40 (393 K) to 70 V (297 K). Average resistivity in the Ohmic low-field region of about 2×10^9 Ω cm (297 K) and 1.5×10^6 Ω cm (393 K), very close to $\rho_{\max}$ at these temperatures, suggests that the entire crystal is depleted at zero bias. Under these conditions, the weak sublinearity noted in both forward and reverse characteristics at high fields may be indicative of an increase in $\rho_{\max}$ due to electron velocity saturation.

F. Interpretation

Both the Ohmic behavior of the forward characteristic up to voltages which may be many times larger than the junction built-in potential and the subsequent sublinear increase of current with voltage are unique features of relaxation-case junctions which have been confirmed by the present work. Resistance in the Ohmic region is larger than that calculated from bulk-resistivity values and does not scale with sample length. The trivial

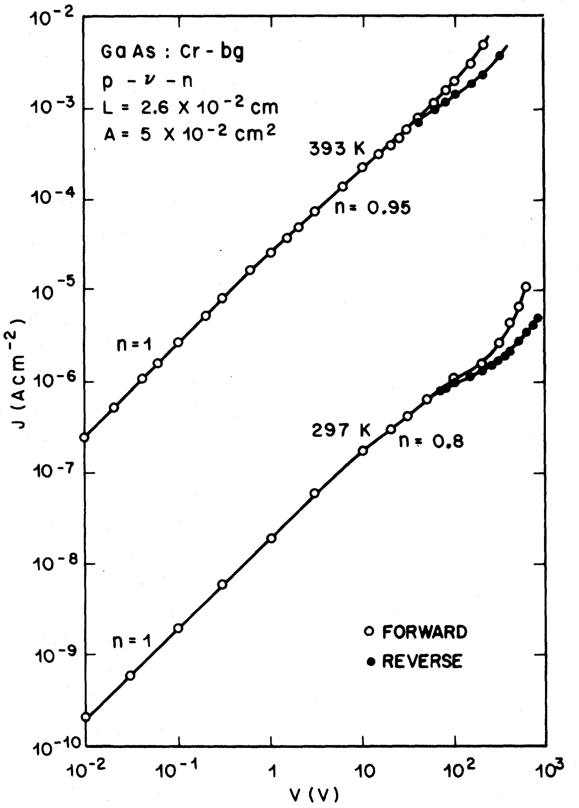

FIG. 5. Current–density–voltage characteristics: p-ν-n diode, Zn–diffused p contact, Sn–doped LPE n contact. Forward and reverse are identical below the voltage where curves are shown to separate.

interpretation according to which the forward resistance would be determined primarily by the series resistance of the ν layer can therefore be excluded. In addition, we note that in such cases a superlinear behavior at high fields, such as that observed for the symmetrical n-ν-n structures (Fig. 1), would be expected. Since the increased resistance is observed in samples with nonrectifying back contacts the results therefore suggest the presence of a high-resistivity layer associated with carrier depletion near the injector contact, consistent with the results of earlier potential probing experiments.[6] In terms of the recombinative-injection model, the carrier depletion results from the injection of holes from the p region into the ν-layer where they recombine away majority electrons.[5] At low injection levels, this hole injection does apparently not appreciably alter the depletion-layer width so that a near-Ohmic characteristic results. The sublinear increase of current with voltage observed at higher injection levels is then attributed[5] to an increase of the depletion layer width by amounts proportional to the total current.

The analysis originally given by van Roosbroeck and Casey[5] thus accounts qualitatively for the main features observed. However, several questions remain regarding this interpretation. First, the assumption is made that current transport in the depletion layer in the vicinity of the maximum resistivity point is predominantly due to drift. The field required to obtain a regime of predominant drift under large forward bias must be associated with the presence of a space-charge doublet. The positive charge in this doublet results mainly from traps that have become occupied or neutralized by the injected minority carriers. This positive charge must be neutralized by a compensating negative space-charge region to effect the transition to the unmodulated semiconductor. The injected region and the compensating space-charge region are separated by a recombination front[5] of near $\rho_{\max}$ resistivity in which current transport changes from hole to electron conduction. It has been pointed out by Kiess and Rose[9] that such a compensating space charge cannot arise from an excess of majority carriers which would be unstable, and hence can also not arise from a trapped charge in quasiequilibrium with the free carriers. Familiar equilibrium concepts regarding trap occupancy can therefore not account for the existence of such space-charge doublet. Second, computer calculations by Döhler and Heyszenau[8] which included diffusion gave no range of sublinear current but rather a superlinear behavior associated with predominant diffusion near the region of maximum resistivity. These calculations, however, assume the characteristic approximation $np = n_i^2$ to hold throughout the sample and thus rule out the existence of a recombination front. It seems clear, however, that diffusion may play an important role and should therefore be included in a complete analysis.

More recently, Popescu and Henisch[28] extended the computer analysis of the transport equation by allowing departures from the $np = n_i^2$ condition. This work confirmed the predicted[5] depletion of majority carriers as a result of the recombinative injection of minority carriers, as well as the existence of a recombination front in which current changes from minority carriers to majority carriers and in which np appreciably exceeds n_i^2. The computed current-voltage characteristics show an extended linear forward region but no or only very weak sublinear behavior. In addition, under forward bias the calculated sample resistance over the region beyond the injection or zero-field plane, is everywhere lower than that evaluated from bulk resistivity.

None of the theories developed so far is thus able to give a satisfactory interpretation of the observed sublinearity in the forward characteristic and of the fact that the sample resistances under either bias are higher than the bulk-resistance value. The computer results,[8,28] which are for no trapping, show transport of the injected minority carriers to be predominantly by diffusion, while the treatment by van Roosbroeck and Casey[5] assumes the existence of a high-field region in which minority carrier transport is primarily by drift. The difference between these two results is directly related to the assumptions made as to the behavior of traps: In the no-trapping case, or in the case where the trap occupancy is everywhere in equilibrium with the free carriers, the stability argument[9] effectively rules out the existence of a high-field region. It is clear, however, that recombination and trapping in relaxation-case materials may differ significantly[3] from the usual lifetime-case behavior and a detailed treatment taking into account the various arrival and trapping rates of carriers may be required to establish the steady-state trap occupancy and charge-distribution profile in the vicinity of the recombination front.

Possible interpretations other than recombinative injection to explain the sublinear behavior observed have been examined. Of the mechanisms leading to resistance increases we can cite here field-dependent capture by Coulomb repulsive centers,[29,30] velocity saturation of electrons due to intervalley scattering,[31] velocity saturation due to acoustoelectric effects,[32] and preferential capture of upper-valley electrons by deep traps.[33] Other observations that may be compared to the present experiments are contact-limited current effects[34] leading to domain formation in GaAs : O and kinetics of current rise in GaAs : O and GaAs : Cr after application of voltage steps.[35]

None of these various alternative mechanisms appear to bear on the observed sublinear behavior or can account for the long near-Ohmic behavior at low forward bias. With regard to the velocity-saturation effects we note that the very long transient times when switching into and out of the sublinear region provide strong evidence against a simple valley-transfer mechanism, which is a very fast process. The long transients rather suggest actual charging and discharging processes and widening and shrinking of space-charge layers. Recent studies[36] on the behavior of relaxation-case diodes under hydrostatic pressure also argue against an explanation of the sublinear forward by a velocity-saturation effect.

It should be noted also that the space-charge layer is of near-maximum resistivity with essentially equal hole and electron contributions. Since only the electrons are affected by the valley transfer, the holes should provide increasing fractions of the total current until the asymptotic condition of predominating hole current at a device resistance twice the low-field value is reached. We may have indeed observed this behavior with Cr-doped devices as discussed in connection with Fig. 5. This effect is predicted and observed to yield a distinguishably different current-voltage characteristic than the one for sublinear behavior under discussion.

V. CONCLUSION

Experiments on technologically well controlled *p-ν-n* structures of oxygen-doped semi-insulating GaAs have shown that the quasi-Ohmic forward characteristic followed by a sublinear range is a reproducible effect which is related to the presence of a high-resistivity space-charge layer adjoining the *p* contact. The experimental results appear to be consistent with the recombinative injection model proposed by van Roosbroeck. However, a more complete theoretical treatment of the relaxation-case behavior predicted for the diode structures studied here is required before the experimental results can be definitely evaluated.

ACKNOWLEDGMENTS

The authors thank W. van Roosbroeck for many critical and detailed discussions, and H. C. Casey, Jr. for his interest and advice during the course of this work. The expert help of P. W. Foy and R. B. Zetterstrom with sample preparation is greatly appreciated. One of them (H. J. Q.) gratefully acknowledges the hospitality of Bell Laboratories during a summer visit with special thanks to G. K. Wertheim and J. A. Giordmaine. They benefitted from discussions with G. H. Döhler, H. Heyszenau, H. Kiess, A. Rose, and F. Stöckmann.

---

*Permanent address: Max-Planck-Institut für Festkörperforschung, 7 Stuttgart 1, Germany.

[1] N. F. Mott and E. A. Davis, *Electronic Processes in Non-Crystalline Materials* (Clarendon, Oxford, 1971).

[2] J. Tauc, *Amorphous and Liquid Semiconductors* (Plenum, New York, 1974).

[3] W. van Roosbroeck, Phys. Rev. Lett. 28, 1120 (1972); J. Non-Cryst. Solids 12, 232 (1973).

[4] W. van Roosbroeck, Phys. Rev. 123, 474 (1961).

[5] W. van Roosbroeck and H. C. Casey, *Proceedings of the 10th International Conference on the Physics of Semiconductors* (U. S. AEC, Springfield, Va., 1970), p. 832; Phys. Rev. B 5 2154 (1972).

[6] H. J. Queisser, H. C. Casey, and W. van Roosbroeck,

Phys. Rev. Lett. **26**, 551 (1971).

[7] H. J. Queisser, in *Solid State Devices*, edited by P. N. Robson (Institute of Physics, Bristol, 1973), p. 145.

[8] G. H. Döhler and H. Heyszenau, Phys. Rev. Lett. **30**, 1200 (1973).

[9] H. Kiess and A. Rose, Phys. Rev. Lett. **31**, 153 (1973).

[10] F. Stöckmann, Phys. Status Solidi (a) **16**, K157 (1973).

[11] L. J. Van der Pauw, Philips Res. Rep. **13**, 1 (1958).

[12] H. C. Casey and M. B. Panish, Trans. AIME **242**, 406 (1968).

[13] D. D. Sell and H. C. Casey, J. Appl. Phys. **45**, 800 (1974).

[14] M. B. Panish and H. C. Casey, J. Appl. Phys. **40**, 163 (1969); C. D. Thurmond, J. Electrochem. Soc. (to be published).

[15] J. L. Moll, *Physics of Semiconductors* (McGraw Hill, New York, 1964).

[16] A. G. Milnes, *Deep Impurities in Semiconductors* (Wiley, New York, 1973).

[17] C. H. Gogh, C. Hilsum, and B. R. Holeman, J. Appl. Phys. **32**, 2069 (1961).

[18] R. W. Haisty, E. W. Mehal, and R. Stratton, J. Phys. Chem. Solids **23**, 829 (1962).

[19] J. S. Blakemore, *Semiconductor Statistics* (Pergamon, New York, 1962).

[20] R. W. Haisty and G. R. Cronin, *Proceedings of the 7th International Conference on the Physics of Semiconductors* (Dunod, Paris, 1964), p. 1161.

[21] H. G. Grimmeiss (private communication); H. E. Grimmeiss and L. A. Ledebo, J. Appl. Phys. **46**, 2155 (1975).

[22] D. V. Lang and R. A. Logan, J. Electron. Mat. (to be published).

[23] D. R. Heath, P. R. Selway, and C. C. Tooke, Brit. J. Appl. Phys. **1**, 29 (1968).

[24] D. Bois and P. Pinard, Phys. Status Solidi (A **7**, 85 (1971).

[25] H. J. Queisser, J. Appl. Phys. **43**, 3893 (1972).

[26] C. T. Sah, L. Forbes, L. I. Rosier, and A. F. Tasch, Solid State Electron, **13**, 759 (1970).

[27] B. V. Tsarenkov, Y. A. Goldberg, E. A. Posse, and S. M. Shulinskaya, Fiz. Tekh. Poluprovodn. **6**, 2392 (1972) [Sov. Phys.-Semicond. **6**, 2003 (1973)].

[28] C. Popescu and H. K. Henisch, Phys. Rev. B **11**, 1563 (1975).

[29] B. K. Ridley and R. G. Pratt, J. Phys. Chem. Solids **26**, 21 (1965).

[30] A. P. Ferro and S. K. Ghandi, J. Appl. Phys. **42**, 4015 (1971).

[31] B. K. Ridley, Brit. J. Appl. Phys. **17**, 595 (1966).

[32] H. Hayakawa, M. Kikuchi and Y. Abe, Jap. J. Appl. Phys. **5**, 734 (1966).

[33] Y. Tokumaru and N. Mikoshiba, Proceedings of the 2nd Conference on Solid State Devices, Tokyo, 1971, (unpublished), p. 107; Jpn. J. Appl. Phys. **11**, 678 (1972).

[34] Y. U. Vorobev, Y. I. Karkhanin, and O. V. Tretyak, Phys. Status Solidi **36**, 499 (1969).

[35] V. A. Brodovoi and N. Z. Derikot, Fiz. Tekh. Poluprovodn. **7**, 108 (1973); **7**, 1431 (1973) [Sov. Phys.-Semicond. **7**, 74 (1973); **7**, 958 (1974)].

[36] W. B. Holzapfel and H. J. Queisser, J. Appl. Phys. **46**, 2810 (1975).